



# Relationship between condensed droplet coalescence and surface wettability



Fuqiang Chu, Xiaomin Wu<sup>\*</sup>, Yi Zhu, Zhiping Yuan

Key Laboratory for Thermal Science and Power Engineering of Ministry of Education, Beijing Key Laboratory for CO<sub>2</sub> Utilization and Reduction Technology, Department of Thermal Engineering, Tsinghua University, Beijing 100084, China

## ARTICLE INFO

### Article history:

Received 25 February 2017

Received in revised form 11 April 2017

Accepted 11 April 2017

### Keywords:

Condensation

Droplet coalescence

Surface wettability

Regional map

Hysteresis number

## ABSTRACT

Droplet condensation, which has better heat transfer performance than film condensation, can improve the efficiency of various engineering applications such as power generation, water harvesting and air conditioning. With the growth of condensed droplets, coalescence among these droplets is certainly taking place. Since the coalescence behavior greatly influences the droplet growth, the relationship between the droplet coalescence and the surface wettability needs to be understood. In this study, condensation experiments on prepared surfaces with various wettability were performed to observe the droplet coalescence behavior. The relationship between the droplet coalescence and the surface wettability was discussed and a regional map was created to classify different droplet coalescence behavior with four regions divided. To make the divided regions understandable, a dimensionless number called the Hysteresis number was first defined to denote the relative importance of the contact angle hysteresis compared to the contact angle for a random surface. Besides the application for analyzing the droplet coalescence behavior, the Hysteresis number can be widely applied for analyzing surface-droplet interactions in various engineering fields with a high value indicating that the contact angle hysteresis plays an important role and cannot be ignored.

© 2017 Elsevier Ltd. All rights reserved.

## 1. Introduction

Condensation, a naturally occurring phenomenon, has various engineering applications such as power generation, air conditioning and desalination [1–3]. For any of these, enhancing the condensation is essential. The most commonly used method is increasing the surface hydrophobicity. It was discovered very early that the droplet condensation on the hydrophobic surface has a better heat transfer performance due to the efficient gravity-driven droplet removal mechanism than the film condensation on the hydrophilic surface [4–6]. In recent years, superhydrophobic surfaces have been suggested to further improve the droplet mobility and then enhance the heat transfer [7,8]. Dietz et al. thought superhydrophobic surfaces allowed the condensed droplets to depart from the surface with a small tilt angle and the resulting decrease in droplet departure size shifted the drop size distribution to smaller radii, which may enhance the condensation heat transfer performance [8].

Besides, the superhydrophobic surfaces with great water repellency have some other advantages. Boreyko and Chen first reported

a self-propelled droplet movement called the droplet jumping during droplet condensation on the superhydrophobic surface [9]. The droplet jumping is triggered by the droplet coalescence, during which the droplet interface connects and deforms with redundant surface energy released to drive the jumping [9]. Their results demonstrated that the droplets were able to leave the surface spontaneously without the help of external forces such as gravity, which indicates that the droplets on the superhydrophobic surface have a greater mobility than imagination. Some researchers then observed the self-propelled droplet jumping on both the natural and artificial superhydrophobic surfaces [10–12] and demonstrated that the jumping-droplet condensation had larger heat transfer coefficient than normal droplet condensation without the droplet jumping [13,14]. In addition to the droplet jumping, another self-propelled droplet movement along the superhydrophobic surface called the droplet sweeping was also observed [15,16]. The droplet sweeping, which is also triggered by the droplet coalescence, is able to self-clean more droplets with larger surface area exposed than the droplet jumping [16], and then may have greater potential in various engineering applications [10,14,17], including the condensation heat transfer enhancement.

That is to say, the condensation performance depends on the condensed droplet mobility to a great extent. In fact, the thermal

<sup>\*</sup> Corresponding author.

E-mail address: [wuxiaomin@mail.tsinghua.edu.cn](mailto:wuxiaomin@mail.tsinghua.edu.cn) (X.M. Wu).

resistances during condensation mainly result from the droplets themselves [18,19]. Droplet with good mobility can be easily shed, resulting in large condensation heat transfer rate. Inspired by the coalescence-induced droplet jumping and sweeping phenomena, we know that the droplet coalescence behavior seems to be a direct reflection of the droplet mobility. As the condensed droplet coalescence is a surface-dependent process, the condensation surface wettability, including both the contact angle and the contact angle hysteresis, influences the droplet coalescence behavior greatly [20]. However, some fundamental questions still need to be determined, such as the exact relationship between the condensed droplet coalescence and the surface wettability, as well as the importance evaluation of the often ignored contact angle hysteresis.

In this study, condensation experiments were conducted on the prepared surfaces with various wettability with condensed droplet coalescence behavior observed and characterized. Then the relationship between the droplet coalescence and the surface wettability was discussed with a regional map created to show the results. In addition, a dimensionless number called the Hysteresis number was first defined to describe the relative importance of the contact angle hysteresis compared to the contact angle for a surface. We hope that, not only for discussing the condensed droplet coalescence behavior on a surface, but also for analyzing other surface-droplet interaction processes such as deicing/defrosting, droplet evaporation and droplet impacting, the Hysteresis number could offer convenience.

## 2. Experimental section

### 2.1. Experimental surfaces

In this study, condensation experiments were conducted on various surfaces with the droplet coalescence behavior observed. Five experimental surfaces with various wettability were prepared using different fabrication methods. Surface wettability was measured using a contact angle goniometer (JC2000C1, China) at room temperature (25 °C) including the apparent contact angle (CA or  $\theta_0$ ) and the contact angle hysteresis (CAH). For each surface, the contact angle was measured by the sessile drop method with 2  $\mu$ L deionized water, its uncertainty of measurement was  $\pm 1^\circ$ . The contact angle hysteresis was the difference between the advancing contact angle ( $\theta_a$ ) and the receding contact angle ( $\theta_r$ ), which were measured by the tilting plate method with the uncertainty of measurement of  $\pm 3^\circ$ .

Surface A (CA = 70° and CAH = 46°) was a bare aluminum surface. Surface B (CA = 90° and CAH = 41°) was obtained by modifying an aluminum surface using a kind of fluoroalkyl silane with low surface energy. Using the chemical etching method, surface C (CA = 126° and CAH = 33°) and surface D (CA = 142° and CAH = 28°) were fabricated through controlling different chemical etching time [21]. Surface E (CA = 160° and CAH = 6°) was fabricated using the chemical etching-deposition method reported in our previous work [22].

### 2.2. Experimental system and conditions

The experimental system used in this research is the same as that in Ref. [23] and we won't do a detailed introduction here. The experimental surfaces were horizontal on the cold side of the semiconductor cooler with the condensation experiments performed in a closed laboratory. The laboratory temperature was measured to be  $20.0 \pm 0.5$  °C with a relative humidity of  $50.0 \pm 2.0\%$ . The cold surface temperature was  $2.0 \pm 0.1$  °C. Images

were captured using an optical microscope equipped with a CCD camera (OLYMPUS DP25, Japan) for top-down imaging.

## 3. Results and discussion

### 3.1. Droplet coalescence behavior on various surfaces

The droplet condensation was mainly divided into two stages with the droplet nucleation at nucleation sites and the initial droplet growth primarily by direct condensation and then by coalescence as the droplets grew larger and as the distances between neighboring droplets became smaller [5]. The droplet coalescence behavior at the second stage of condensation was observed on the experimental surfaces. Fig. 1 shows the droplet coalescence features on five experimental surfaces. On surface A, which is a hydrophilic surface, condensed droplets always have irregular shapes with the coalesced droplet also maintaining an irregular shape (see the marked area in Fig. 1(a)). On surface B, as the marked area in Fig. 1(b) shows, suborbicular droplets coalesce and the coalesced droplet usually shows an elliptical triple-phase line. On surface C, droplets grow uniformly and the droplet keeps spherical shape after coalescence. The coalesced droplet is immobile and remains in situ (see the marks in Fig. 1(c)). On surface D, as the marks in Fig. 1(d) show, coalesced droplets are also spherical and most of the droplet coalescences are immobile, but the coalescence-induced droplet jumping and droplet sweeping begin to occur occasionally. While on surface E, which is a superhydrophobic surface, the droplet coalescence features become quite different. Coalescence among droplets easily triggers self-propelled droplet movements such as droplet jumping and droplet sweeping. As Fig. 1(e-i) shows, the droplet jumping occurs frequently with the droplets on the surface updated quickly. The large-scale droplet sweeping triggered by coalescence among droplets with different sizes and asymmetric locations also occurs easily (see Fig. 1(e-ii)), self-cleaning more droplets and exposing larger surface area than the droplet jumping [16]. Compared with the occasional self-propelled droplet movements on surface D, the self-propelled droplet movements on surface E are so frequent that the normal growth of the condensed droplets are disturbed with more scattered positional distributions and larger size differences [23].

According to the minimal energy principle and the Young's equation, droplet tends to keep spherical shape with the minimal surface energy on a surface. As mentioned above, the coalesced droplets on surface A and B cannot shrink smoothly to reach the minimum energy state, which means that the triple-phase lines of the coalesced droplets pin on the surface strongly with large movement resistances. On surface C and D, which are hydrophobic surfaces, the droplet coalescences become smoothly with the coalesced droplets keeping spherical shapes, and even the self-propelled droplet movements can be triggered by the droplet coalescence on surface D, although the frequency is extremely low. On the superhydrophobic surface E, the self-propelled droplet movements occur much more frequently with a half of droplet coalescences able to trigger self-propelled droplet movements [16]. Thus, we demonstrated that, from surface A to surface E (surface contact angle is larger and contact angle hysteresis is smaller), the droplet coalescence becomes more smoothly with more spherical shapes, the droplet mobility also becomes better with self-propelled phenomena triggered.

### 3.2. Regional map for the relationship between the droplet coalescence and the surface wettability

Since the droplet coalescence is a surface-droplet interaction process, to understand further mechanism, the relationship

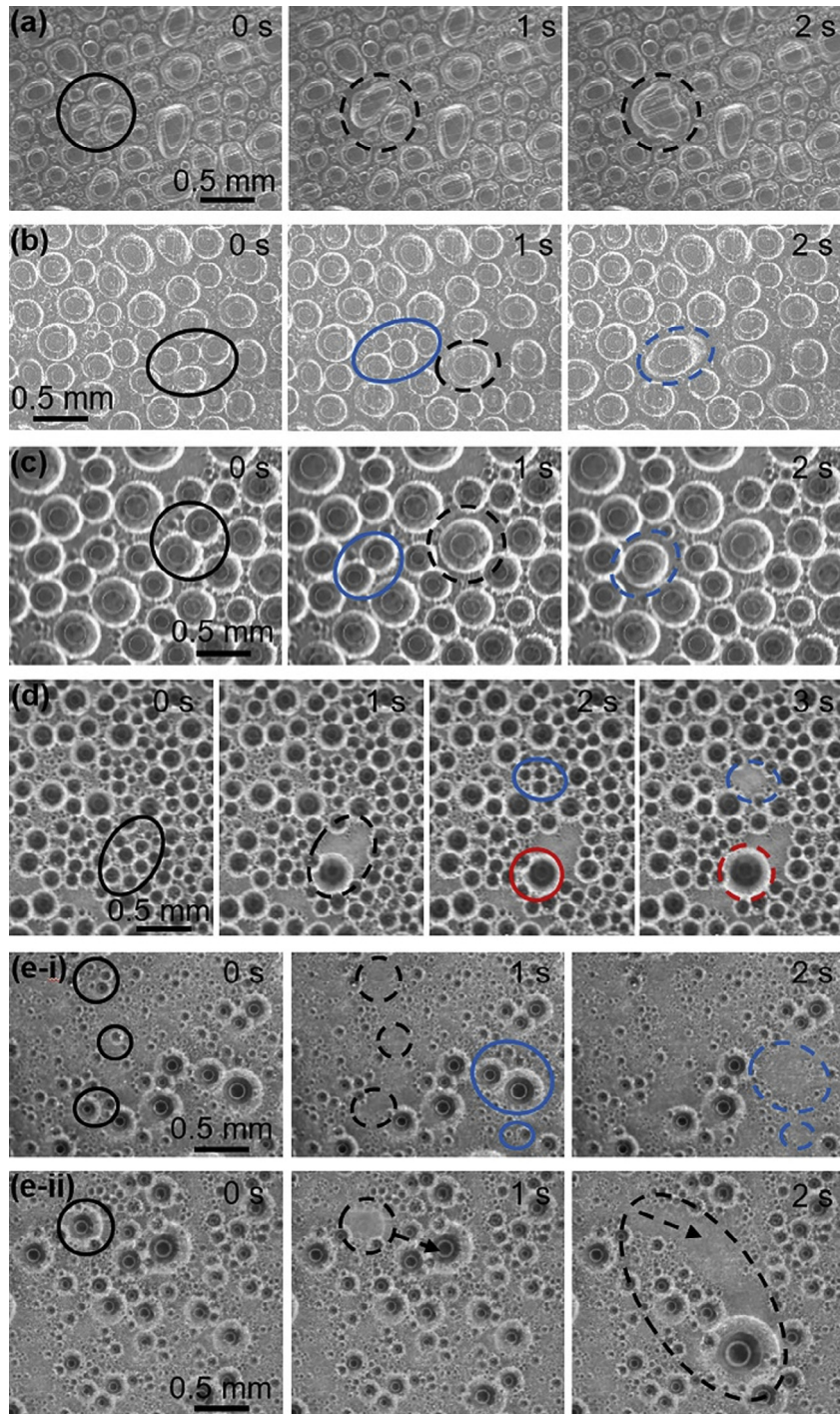


**Fig. 1.** Droplet coalescence features on various surfaces. (a) Surface A: condensed droplets have irregular shapes with the coalesced droplet also maintaining an irregular shape; (b) Surface B: suborbicular droplets coalesce and the coalesced droplet usually shows an elliptical triple-phase line; (c) Surface C: coalesced droplet has spherical triple-phase line, and the droplet coalescence is immobile with the coalesced droplet remaining in situ. (d) Surface D: coalesced droplets are spherical with most droplet coalescences immobile, but the droplet jumping and small-scale droplet sweeping occur occasionally. (e) Surface E: (i) the self-propelled droplet jumping triggered by droplet coalescence occurs frequently with droplets on the surface updated quickly and (ii) the self-propelled droplet sweeping triggered by coalescence among droplets with different sizes and asymmetric locations occurs easily.

between the droplet coalescence and the surface wettability was discussed theoretically. Fig. 2(a) shows the droplet coalescence process on a random surface. During the coalescence process, the droplet experiences serious deformations both on the interface and on the triple-phase line with several energy forms involved and several forces acting [24–29]. From the point of energy, there are surface energy, viscous dissipation, gravitational potential energy and energy dissipation on the triple-phase lines interacting

during the droplet coalescence process. From the point of force, except for the surface tension, the internal viscous force and the gravity, there are resistances existing on the advancing triple lines ( $F_{adv}$ ) and the receding triple lines ( $F_{rec}$ ) due to the surface contact angle hysteresis.

When neglecting the influence of the gravity for droplets whose sizes are much less than the capillary length (for water, the capillary length is about 2.7 mm), the contact angle mainly determines

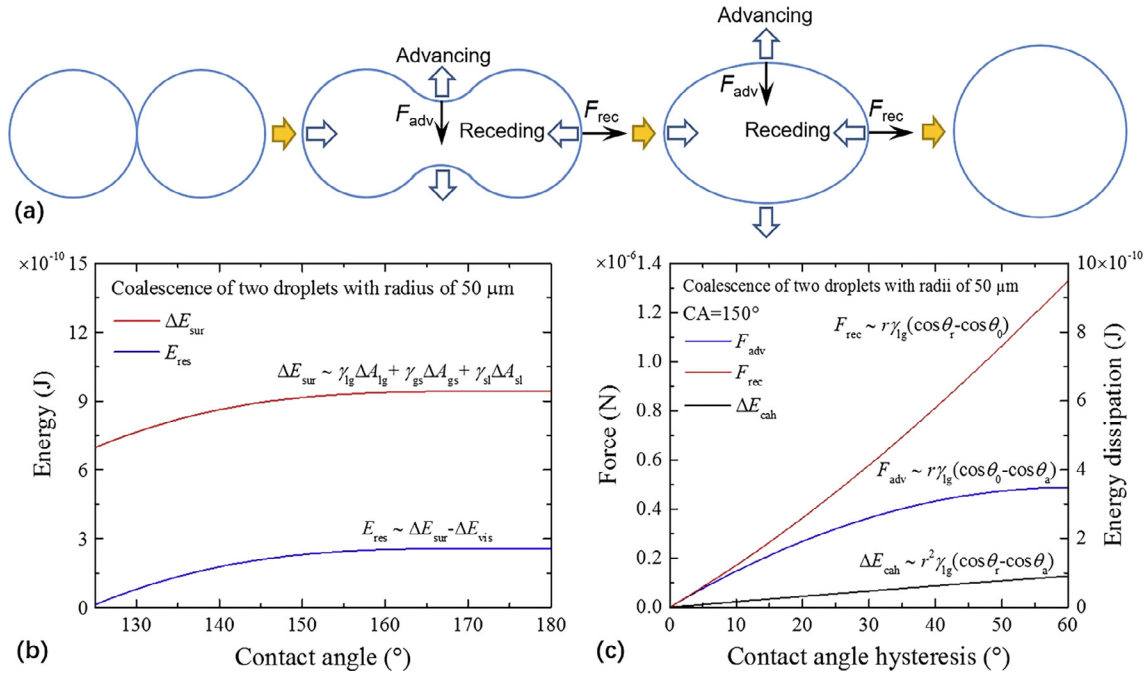


**Fig. 2.** (a) The schematic diagram of a two-droplet coalescence (top view). (b) The contact angle determines the amount of the released surface energy ( $\Delta E_{sur}$ ) and the residual energy ( $E_{res}$ ) after overcoming the viscous dissipation ( $\Delta E_{vis}$ ). With increasing contact angle, both  $\Delta E_{sur}$  and  $E_{res}$  increase. (c) The contact angle hysteresis determines the resistances ( $F_{adv}$  and  $F_{rec}$ ) and the energy dissipation ( $\Delta E_{cch}$ ) existing on the triple-phase lines with both of them increasing with increasing contact angle hysteresis.

the amount of the released surface energy ( $\Delta E_{sur}$ ) and the residual energy ( $E_{res}$ ) after overcoming the viscous dissipation ( $\Delta E_{vis}$ ). The detailed equations for calculating  $\Delta E_{sur}$  and  $\Delta E_{vis}$  are given in Refs. [24–26]. According to these equations, using the coalescence of two droplets with radii of 50  $\mu\text{m}$  as an example, the released surface energy and the residual energy were calculated. As Fig. 2(b) shows, with increasing contact angle, both  $\Delta E_{sur}$  and  $E_{res}$  increase, which means there is increasing power to drive the coalesced droplet. Moreover, for coalescence of droplets with certain radii, there is a threshold value of the contact angle. When the actual contact angle is less than the threshold value, there is no residual energy left. At this time, we may say the contact angle is not large enough. For example, the threshold value is about  $125^\circ$  for coalescence of two droplets with 50  $\mu\text{m}$  radii.

Different with the contact angle, the contact angle hysteresis determines the resistances ( $F_{adv}$  and  $F_{rec}$ ) and the energy dissipation ( $\Delta E_{cch}$ ) existing on the triple-phase lines. The resistances and energy dissipation existing on the triple-phase lines can be evaluated by equations in Refs. [27–29]. With the simple assumption that  $0.5(\theta_a + \theta_r) = \theta_0$  [30,31], the resistances and the energy dissipation on the triple-phase lines were calculated in Fig. 2(c). As seen, for larger contact angle hysteresis, the resistances on the triple-phase line get larger with more residual energy required to overcome the energy dissipation.

In a word, the contact angle decides whether there is residual energy after coalescence, while the contact angle hysteresis decides the resistances and the energy dissipation on the triple-phase line when the coalesced droplet shrinks or moves. To show the relationship between the droplet coalescence behavior and the surface wettability more clearly, a regional map is created in Fig. 3 with the horizontal axis being the contact angle and the vertical axis representing the contact angle hysteresis. On the map, four regions are divided. Region I represents surface with small contact angle but large contact angle hysteresis. There is no residual energy left after droplet coalescence on surfaces in this region, and the surface tension cannot overcome the resistances completely on the triple-phase line, so the coalesced droplets pin

strongly with elliptical even irregular shapes. Most untreated metal surfaces such as surface A and B belong to this region. Region II represents surface with small contact angle and small contact angle hysteresis. Although there is no residual energy left after droplet coalescence, there is barely resistance on the triple-phase line with the coalesced droplet maintaining circular triple-phase line. The droplets cannot move spontaneously but they are easily driven when there is applied force, such as wind or gravity. Although we didn't prepare an experimental surface belonging to Region II, we could find examples which are in Region II. For example, the lubricant-impregnated surface (CA is about  $67^\circ$  and CAH is about  $3^\circ$ ) prepared by Anand et al. is an example with the condensed droplets on the surface coalesce and keep spherical shapes [32]. The slippery surfaces of pitcher plants [33,34] are also typical examples in Region II. Region III represents surface with large contact angle and large contact angle hysteresis, on which the residual energy is used to overcome the energy dissipation on the triple-phase line. After the triple-phase line shrinks into round shape finally, the residual energy runs out with the coalesced droplet staying at pinning state. The surface C and those rose petal surfaces [35,36] are typical examples belonging to Region III. Region IV represents surface with large contact angle but small contact angle hysteresis. On surfaces in region IV, the residual energy of the coalesced droplet is enough and the energy dissipation on the triple-phase line is negligible, so the self-propelled droplet movements are easily triggered by droplet coalescence. The lotus surface [37] and other superhydrophobic surfaces such as surface E belong to this region.

### 3.3. The Hysteresis number

From above discussion, we know the surface contact angle and the contact angle hysteresis codetermine the droplet coalescence behavior with different combinations resulting in different results. However, it must be emphasized that the “large” or “small” of the contact angle and the contact angle hysteresis are relative concepts. We determine whether or not the contact angle is large by calculating the residual energy ( $E_{res}$ ). If the residual energy is more

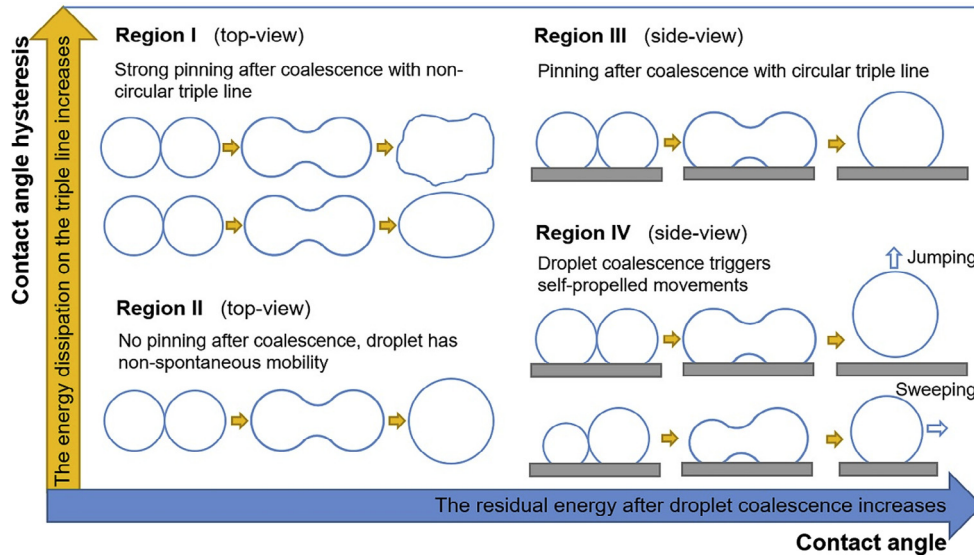


**Fig. 3.** The regional map for the relationship between the droplet coalescence behavior and the surface wettability. Region I represents surface with small CA but large CAH, and the coalesced droplet pins on the surface strongly with elliptical even irregular triple-phase line. Region II represents surface with small CA and small CAH. The coalesced droplet with slippery circular triple-phase line has non-spontaneous mobility and easily moves when there is applied force. Region III represents surface with large CA and large CAH, and the coalesced droplet has circular triple-phase line but keeps pinning state. Region IV represents surface with large CA but small CAH. In region IV, self-propelled droplet movements such as droplet jumping and droplet sweeping are easily triggered by the droplet coalescence.

than zero, the contact angle is thought to be large. For a known contact angle, we determine whether the contact angle hysteresis is large or small by a new defined dimensionless number in this study.

Inspired by above energy analysis, a dimensionless number called Hysteresis number is defined as the ratio of the dimensionless energy dissipation on the triple-phase line ( $\cos\theta_r - \cos\theta_a$ ) to the dimensionless surface energy ( $1 - \cos\theta_0$ ) of a droplet.

$$\text{Hysteresis number} = k \frac{\cos\theta_r - \cos\theta_a}{1 - \cos\theta_0} \quad (1)$$

where  $k$  is a dimensionless correction factor. With the assumption that  $0.5(\theta_a + \theta_r) = \theta_0$  and  $k$  set to be 0.5, the Hysteresis number is further simplified as

$$\text{Hysteresis number} = \frac{\sin \frac{\text{CAH}}{2}}{\tan \frac{\text{CA}}{2}} \quad (2)$$

As the Eq. (2) shows, the equation of the Hysteresis number is concise with a clear physical meaning which denotes the relative importance of the contact angle hysteresis compared to the contact

angle for a surface. According to Eq. (2), the definition domain of the Hysteresis number is from 0 to 2. A high value (hypothetically more than 0.1) of the Hysteresis number indicates that the contact angle hysteresis plays an important role and cannot be ignored when discussing surface-droplet interaction processes, such as deicing/defrosting, droplet evaporation and droplet impacting [17,38–40].

To further explain the Hysteresis number, a contour map of the Hysteresis number is drawn in Fig. 4. For droplet coalescence with 50  $\mu\text{m}$  radii, Region I – IV were divided on the contour map with the boundary lines (dashed lines) being  $E_{res} = 0$  and Hysteresis number = 0.1. According to Eq. (2), the Hysteresis numbers for the experimental surfaces were calculated. As shown in Fig. 4, the Hysteresis number for surface A is about 0.56 and for surface B is about 0.35, which means that the contact angle hysteresis is quite large compared to the contact angle, so surface A and surface B with small contact angles but large contact angle hysteresis belongs to Region I. The Hysteresis number of the lubricant-impregnated surface prepared by Anand et al. [32] is about 0.04, so this surface belongs to Region II. The Hysteresis number for surface C is about 0.14, indicating that surface C belongs to Region III.

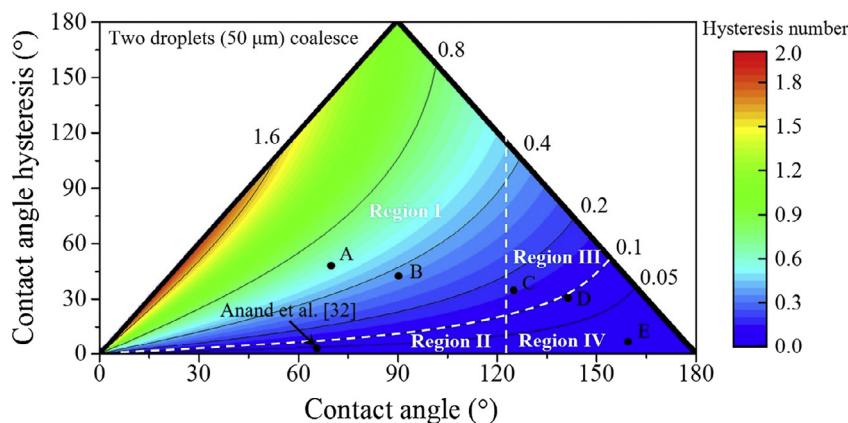


**Fig. 4.** The contour map of the Hysteresis number and the region division on the contour map. The locations of the experimental surfaces are also shown on the contour map.

For surface D, the Hysteresis number is nearly 0.1. As the Hysteresis number = 0.1 is a relatively loose boundary, surface D locates at the transition region between Region III and Region IV. The Hysteresis number for surface E is less than 0.01 with negligible contact angle hysteresis compared to the very large contact angle, so surface E belongs to Region IV. We qualitatively determined the locations of the experimental surfaces on the regional map in Fig. 3 in the last section, while the quantitative results in Fig. 4 are consistent with those in Fig. 3, which indicates the usability and the reasonability of the Hysteresis number.

#### 4. Conclusions

In summary, condensation experiments on five prepared surfaces with various wettability were performed to observe and classify the droplet coalescence behavior. The relationship between the droplet coalescence and the surface wettability was discussed with a regional map, on which four regions were divided, created. On the map, region I represents surface with small contact angle but large contact angle hysteresis, where the coalesced droplet pins strongly with irregular shapes and bad mobility. Region II represents surface with small contact angle and small contact angle hysteresis, where the coalesced droplet maintains circular triple-phase line and has non-spontaneous mobility. Region III represents surface with large contact angle and large contact angle hysteresis, where the coalesced droplet has circular triple-phase line but keeps pinning state. Region IV represents surface with large contact angle but small contact angle hysteresis, where the self-propelled droplet motion is easily triggered by the droplet coalescence. Actually, the “large” or “small” of the contact angle and the contact angle hysteresis are relative concepts. We determine whether or not the contact angle is large by calculating the residual energy, and we determine whether or not the contact angle hysteresis is large for a known contact angle by the Hysteresis number. The Hysteresis number, which is first defined in this study, denotes the relative importance of the contact angle hysteresis compared to the contact angle for a surface. The Hysteresis number can be applied in various engineering fields involving surface-droplet interactions, such as deicing/defrosting, droplet evaporation and droplet impacting.

#### Acknowledgements

This work was supported by the National Natural Science Foundation of China (No. 51476084), the Tsinghua University Initiative Scientific Research Program (No. 20131089319) and the National Natural Science Fund for Creative Research Groups (No. 51621062).

#### References

- [1] J.M. Beér, High efficiency electric power generation: the environmental role, *Prog. Energy Combust. Sci.* 33 (2) (2007) 107–134.
- [2] L. Pérez-Lombard, J. Ortiz, C. Pout, A review on buildings energy consumption information, *Energy Build.* 40 (3) (2008) 394–398.
- [3] A.D. Khawaji, I.K. Kutubkhanah, J.-M. Wie, Advances in seawater desalination technologies, *Desalination* 221 (1–3) (2008) 47–69.
- [4] G.A. O'Neill, J.W. Westwater, Dropwise condensation of steam on electroplated silver surfaces, *Int. J. Heat Mass Transfer* 27 (9) (1984) 1539–1549.
- [5] J.W. Rose, Dropwise condensation theory and experiment: a review, *Proc. Inst. Mech. Eng., Part A: J. Power Energy* 216 (2) (2002) 115–128.
- [6] R. Wen, Q. Li, J. Wu, G. Wu, W. Wang, Y. Chen, X. Ma, D. Zhao, R. Yang, Hydrophobic copper nanowires for enhancing condensation heat transfer, *Nano Energy* 33 (2017) 177–183.
- [7] C.-H. Chen, Q. Cai, C. Tsai, C.-L. Chen, G. Xiong, Y. Yu, Z. Ren, Dropwise condensation on superhydrophobic surfaces with two-tier roughness, *Appl. Phys. Lett.* 90 (17) (2007) 173108.
- [8] C. Dietz, K. Rykaczewski, A.G. Fedorov, Y. Joshi, Visualization of droplet departure on a superhydrophobic surface and implications to heat transfer enhancement during dropwise condensation, *Appl. Phys. Lett.* 97 (3) (2010) 033104.
- [9] J. Boreyko, C.-H. Chen, Self-propelled dropwise condensate on superhydrophobic surfaces, *Phys. Rev. Lett.* 103 (18) (2009) 184501.
- [10] K.M. Wisdom, J.A. Watson, X. Qu, F. Liu, G.S. Watson, C.H. Chen, Self-cleaning of superhydrophobic surfaces by self-propelled jumping condensate, *Proc. Natl. Acad. Sci. U. S. A.* 110 (20) (2013) 7992–7997.
- [11] C. Lv, P. Hao, Z. Yao, Y. Song, X. Zhang, F. He, Condensation and jumping relay of droplets on lotus leaf, *Appl. Phys. Lett.* 103 (2) (2013) 021601.
- [12] K. Yanagisawa, M. Sakai, T. Isobe, S. Matsushita, A. Nakajima, Investigation of droplet jumping on superhydrophobic coatings during dew condensation by the observation from two directions, *Appl. Surf. Sci.* 315 (2014) 212–221.
- [13] N. Miljkovic, R. Enright, Y. Nam, K. Lopez, N. Dou, J. Sack, E.N. Wang, Jumping-droplet-enhanced condensation on scalable superhydrophobic nanostructured surfaces, *Nano Lett.* 13 (1) (2013) 179–187.
- [14] N. Miljkovic, E.N. Wang, Condensation heat transfer on superhydrophobic surfaces, *MRS Bull.* 38 (05) (2013) 397–406.
- [15] G.S. Watson, L. Schwarzkopf, B.W. Cribb, S. Myhra, M. Gellender, J.A. Watson, Removal mechanisms of dew via self-propulsion off the gecko skin, *J. R. Soc. Interface* 12 (105) (2015) 20141396.
- [16] F. Chu, X. Wu, B. Zhu, X. Zhang, Self-propelled droplet behavior during condensation on superhydrophobic surfaces, *Appl. Phys. Lett.* 108 (19) (2016) 194103.
- [17] J. Lv, Y. Song, L. Jiang, J. Wang, Bio-inspired strategies for anti-icing, *ACS Nano* 8 (4) (2014) 3152–3169.
- [18] S. Kim, K.J. Kim, Dropwise condensation modeling suitable for superhydrophobic surfaces, *J. Heat Transfer* 133 (8) (2011) 081502.
- [19] B. Qi, J. Wei, L. Zhang, H. Xu, A fractal dropwise condensation heat transfer model including the effects of contact angle and drop size distribution, *Int. J. Heat Mass Transfer* 83 (2015) 259–272.
- [20] K. Sefiane, M.E.R. Shanahan, M. Antoni, Wetting and phase change: opportunities and challenges, *Curr. Opin. Colloid Interface Sci.* 16 (4) (2011) 317–325.
- [21] F.Y. Lv, P. Zhang, Fabrication and characterization of superhydrophobic surfaces on aluminum alloy substrates, *Appl. Surf. Sci.* 321 (2014) 166–172.
- [22] F. Chu, X. Wu, Fabrication and condensation characteristics of metallic superhydrophobic surface with hierarchical micro-nano structures, *Appl. Surf. Sci.* 371 (2016) 322–328.
- [23] F. Chu, X. Wu, Q. Ma, Condensed droplet growth on surfaces with various wettability, *Appl. Therm. Eng.* 115 (2017) 1101–1108.
- [24] Y. Nam, H. Kim, S. Shin, Energy and hydrodynamic analyses of coalescence-induced jumping droplets, *Appl. Phys. Lett.* 103 (16) (2013) 161601.
- [25] X. Liu, P. Cheng, X. Quan, Lattice Boltzmann simulations for self-propelled jumping of droplets after coalescence on a superhydrophobic surface, *Int. J. Heat Mass Transfer* 73 (2014) 195–200.
- [26] X. Liu, P. Cheng, 3D multiphase lattice Boltzmann simulations for morphological effects on self-propelled jumping of droplets on textured superhydrophobic surfaces, *Int. Commun. Heat Mass Transfer* 64 (2015) 7–13.
- [27] B. Peng, S. Wang, Z. Lan, W. Xu, R. Wen, X. Ma, Analysis of droplet jumping phenomenon with lattice Boltzmann simulation of droplet coalescence, *Appl. Phys. Lett.* 102 (15) (2013) 151601.
- [28] Y. Nam, D. Seo, C. Lee, S. Shin, Droplet coalescence on water repellent surfaces, *Soft Matter* 11 (1) (2015) 154–160.
- [29] Y. Cheng, J. Xu, Y. Sui, Numerical investigation of coalescence-induced droplet jumping on superhydrophobic surfaces for efficient dropwise condensation heat transfer, *Int. J. Heat Mass Transfer* 95 (2016) 506–516.
- [30] R.D. Schulze, W. Possart, H. Kamusewitz, C. Bischof, Young's equilibrium contact angle on rough solid surfaces. Part I. An empirical determination, *J. Adhesion Sci. Technol.* 3 (1) (1989) 39–48.
- [31] A. Marmur, Soft contact: measurement and interpretation of contact angles, *Soft Matter* 2 (1) (2006) 12–17.
- [32] S. Anand, A.T. Paxson, R. Dhiman, J.D. Smith, K.K. Varanasi, Enhanced condensation on lubricant-impregnated nanotextured surfaces, *ACS Nano* 6 (11) (2012) 10122–10129.
- [33] H.F. Bohn, W. Federle, Insect aquaplaning: nepenthes pitcher plants capture prey with the peristome, a fully wettable water-lubricated anisotropic surface, *Proc. Natl. Acad. Sci. U. S. A.* 101 (39) (2004) 14138–14143.
- [34] K.C. Park, P. Kim, A. Grinthal, N. He, D. Fox, J.C. Weaver, J. Aizenberg, Condensation on slippery asymmetric bumps, *Nature* 531 (7592) (2016) 78–82.
- [35] L. Feng, Y. Zhang, J. Xi, Y. Zhu, N. Wang, F. Xia, L. Jiang, Petal effect: a superhydrophobic state with high adhesive force, *Langmuir* 24 (8) (2008) 4114–4119.
- [36] B. Bhushan, M. Nosonovsky, The rose petal effect and the modes of superhydrophobicity, *Phil. Trans. R. Soc. A* 368 (1929) (2010) 4713–4728.
- [37] W. Barthlott, C. Neinhuis, Purity of the sacred lotus, or escape from contamination in biological surfaces, *Planta* 202 (1) (1997) 1–8.
- [38] F. Chu, X. Wu, L. Wang, Dynamic melting of freezing droplets on ultraslippery superhydrophobic surfaces, *ACS Appl. Mater. Interfaces* 9 (2017) 8420–8425.
- [39] L. Lin, H. Peng, G. Ding, Influence of oil concentration on wetting behavior during evaporation of refrigerant–oil mixture on copper surface, *Int. J. Refrig.* 61 (2016) 23–36.
- [40] G. Liang, I. Mudawar, Review of drop impact on heated walls, *Int. J. Heat Mass Transfer* 106 (2017) 103–126.